Cratering and plastic deformation in polystyrene induced by MeV heavy ions: Dependence on the molecular weight

L. S. Farenzena* and R. P. Livi
Instituto de Física, Universidade Federal do Rio Grande do Sul, Caixa Postal 15051, 91501-970 Porto Alegre, RS, Brazil

M. A. de Araújo
Instituto de Química, Universidade Federal do Rio Grande do Sul, 91501-970, Porto Alegre, RS, Brazil

G. Garcia Bermudez
U. A. de Fisica, Laboratório TANDAR, Comision Nacional de Energia Atomica, 1429 Buenos Aires, Argentina

R. M. Papaléo
Faculdade de Física, Pontifícia Universidade Católica do Rio Grande do Sul, 90619-900, Porto Alegre, RS, Brazil
(Received 29 August 2000; published 20 February 2001)

Cratering and plastic deformation induced by individual MeV ions on the surface of polystyrene thin films of different molecular weights (M_w) (from 3250 to 2×10^7u) are investigated using scanning force microscopy. 20 MeV, 85 MeV and 197 MeV gold ions are used to bombard the targets at grazing incidence (79° to the surface normal). Induced surface tracks consist of an elliptical crater followed by a hillock elongated in the direction of the ion incidence. For a given ion energy, the crater size is largest on the lowest M_w film. Crater dimensions are systematically reduced on films of heavier macro-molecules, up to a molecular weight of about 1.6×10^5u. For $M_w>1.6\times10^5u$, the crater size remains approximately constant. The difference observed for the lateral dimensions of the craters are about 50% when comparing the lowest and the highest M_w films at a fixed energy. The observed saturation of the crater size for high M_w values coincides with the onset of entanglement effects in the polymer, which influences the viscosity and the compliance of the material. Moreover, the curve of the crater size versus M_w follows the same trend as the reciprocal viscosity (η^{-1}) versus M_w, indicating that the viscosity is governing the final lateral dimensions of the craters. The hillock dimensions present a weak dependence on M_w, above a threshold at $3250u$. The different behavior observed for craters and hillocks is discussed based on the viscoelastic properties of the polymer at different M_w and on the transient heating occurring close to the ion impact site.

DOI: 10.1103/PhysRevB.63.104108 PACS number(s): 79.20.Rf, 61.80.Jh

I. INTRODUCTION

When fast ions interact with thin solids the energy is deposited mostly in the form of electronic excitations, through the nearly straight path of the ion into the target. In insulators, such electronic energy can be rapidly converted into atomic motion, creating defects along a cylindrical region, called *latent track*.[1–3] Near the vacuum/solid interface, deformation of the surface and ejection of material occurs, resulting in the formation of a crater and/or a raised rim or tail (hillock).[4] These surface features are often referred to as *surface tracks*. For polymers, the ejected material can be very diverse, including intact molecules, molecular fragments, and highly reorganized species (e.g., carbon clusters).[5,6] The remaining material in the bulk can be strongly modified near the ion path,[7–10] but few tens of nanometers from the impact center, the deposited energy density is too low to induce significant chemical rearrangements.[10,6]

In recent years, the size and shape of the surface tracks, mostly produced at grazing incidence angles,[11–15,4,16–19] have been investigated with scanning force microscopy (SFM). The use of this technique allows evaluation of the total sputtering yield in single ion events[16,11] and the study of basic ion-solid interactions.[12,20] An inherent limitation of measuring sputtering yields from crater volumes is the dependence of the measured dimensions on the SFM tip shape and on tip-surface interaction forces. However, tip convolution effects are not relevant whenever *relative* changes in the measured dimensions are involved. This was the case in many important experiments reported in the literature, such as the scalings of surface track dimensions with the stopping power,[21] ion velocity,[11] incidence angle,[20,13] and target temperature.[22] Eriksson *et al.*[12] studied surface tracks of MeV ions on organic materials with different molecular weights, but distinct chemical structures. In this work a systematic study of surface tracks in an organic polymer [polystyrene (PS)] is performed for a wide range of molecular weights, keeping the chemical structure fixed. The crater and hillock formation processes are discussed, and correlated with the viscoelastic properties of the polymer.

II. EXPERIMENT

PS powder of different molecular weights, from 3250 to 2×10^7u, nearly monodisperse, were used to prepare the targets. Average molecular weights M_w and polydispersity given by the manufacturer (Polymer Standards Service, USA) and the glass transition temperatures (T_g), measured

TABLE I. Average molecular weight (M_w), polydispersity (M_w/M_n), and glass transition temperature (T_g) of the used PS powder.

$M_w(u)$	M_w/M_n	T_g (°C)
3250	1.05	81.0
6600	1.04	
9250	1.03	98.6
16 700	1.03	
42 000	1.03	106.0
68 000	1.03	108.3
160 000	1.03	109.4
420 000	1.03	109.7
1 200 000	1.05	
3 000 000	1.07	
20 000 000		

for some M_w, are shown in Table I. Thin films were prepared by spin coating, using Si substrates and a PS/xylene or toluene solution. The concentration of the solution and the spinner velocity were slightly different for different molecular weights in order to obtain a flat surface and thickness around 150 nm. The roughness of the surfaces, in a 500-nm^2 scan area, was around 0.3 nm. The thicknesses of the films were determined by two different means: (a) non-Rutherford elastic α-scattering, using 3.5-MeV α particles and measuring the carbon signal depth profile (the beam was aligned at 45° to the normal in order to improve the depth resolution) and (b) by imaging by SFM the film surface containing a previously made scratch and measuring the step between the silicon substrate and the polymer film. The scratches were made using a stainless-steel surgical blade and the width of the scratches varied from 10 to 30 μm. The thicknesses measured via the two methods agree within 10%. The glass transition temperature (T_g) of the polymers was determined by differential scanning calorimetry (Polymer Laboratories) at a heating rate of 20 °C/min.

Bombardments were performed at the Porto Alegre HVEE 3 MV Tandetron accelerator (20-MeV $^{197}Au^{7+}$) and at the Buenos Aires 20 MV Tandar accelerator (85-MeV $^{197}Au^{9+}$ and 197-MeV $^{197}Au^{20+}$) at a fixed impact angle (79° to the surface normal) and with an irradiation fluence around 3×10^9 cm^{-2} and vacuum around 10^{-6} Torr.

Irradiated targets were analyzed by SFM using a Nanoscope IIIa equipment (Digital Instruments) in air (humidity $\approx$60–70 %) in the intermittent contact mode [Tapping Mode^{TM}, (TM-SFM)] with Nanoprobe^{TM} Si tips (with nominal radius of curvature 10 nm and cone angle 36°) and Nanosensors SuperSharpSilicon tips (with nominal radius of curvature 2 nm and cone angle 20°). Further details on microscope operation and imaging quality are presented later in the text.

III. RESULTS AND DISCUSSION

A. Image analysis

Figure 1 shows surface tracks in PS ($M_w=160\,000u$) due to a bombardment with 197-MeV $^{197}Au^{20+}$. Figure 1(a) is a SFM topographic image where five induced surface tracks can be seen. Each one consists of a crater followed by a hillock elongated in the direction of the ion incidence. Sections of a surface track along the incidence direction (1-1′) and perpendicular to the ion direction (2-2′) are given in Figs. 1(c) and 1(e), respectively. The dimensions of the in-

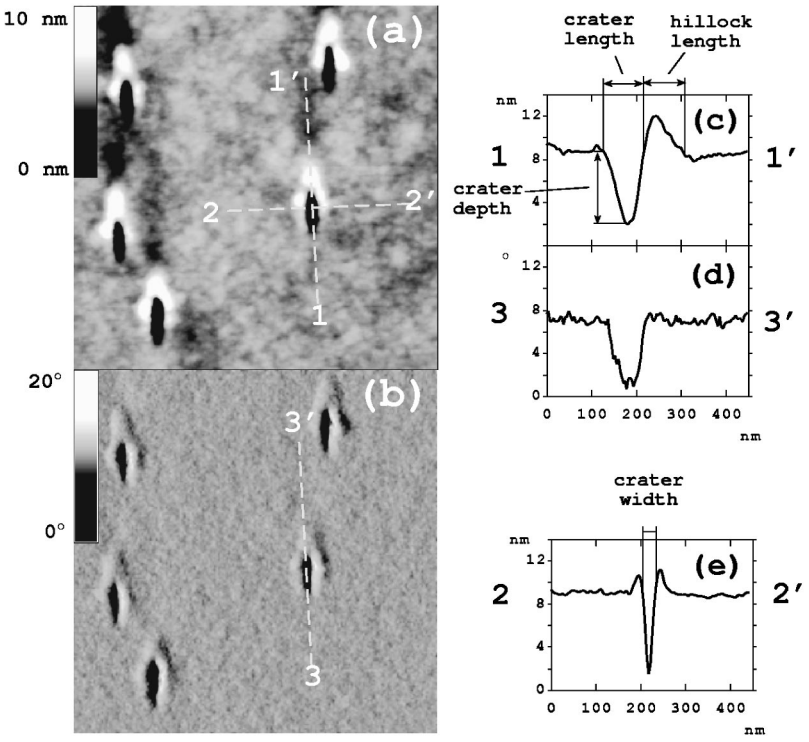

FIG. 1. TM-SFM images of surface tracks in PS targets ($M_w=160\,000u$) bombarded with 197 MeV $^{197}Au^{20+}$, incident along the 1-1′ line at 79° to the surface normal. (a) Topography of the sample showing five induced surface tracks, (b) phase contrast image relative to the same region showed in (a), (c) section on the topographic image along a surface track (1-1′ line), (d) section on the phase image over the same region showed in (c) (3-3′ line), and (e) section perpendicular to a crater (2-2′).

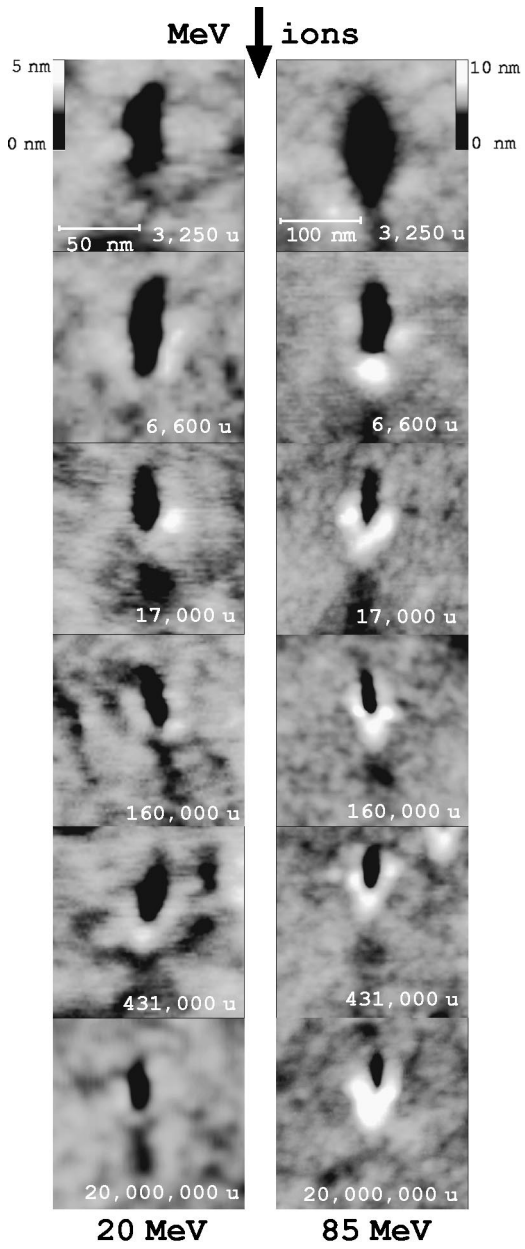

FIG. 2. SFM images of surface tracks induced on PS targets by 20-MeV $^{197}Au^{7+}$ and 85-MeV $^{197}Au^{9+}$ ions for different polymer molecular weights.

duced defects (crater length, width, and depth, and hillock length and height) were determined as shown in these figures.

Figure 1(b) is the phase image corresponding to the topography shown in Fig. 1(a). The interpretation of the phase contrast is yet a subject of discussion, but there are convincing experiments showing that for constant cantilever amplitude, the phase shift is proportional to the tip-sample energy dissipation, being sensitive to variations in properties like the elastic modulus, adhesion, and damping.[23,24] The large phase shift observed in Fig. 1(d) in the interior of the crater appears to be due to a change of elastic modulus of the damaged material in the center of the impact. However, the radius of curvature of the tip and the sample can also contribute to a phase shift.[25] The reduced curvature radius can be altered via the topography of the sample, being presumably, responsible for the contrast in phase images observed in the boundaries of the hillocks and can also contribute to the phase shift observed in the region inside the crater. On the top of the hillock, however, no changes in the phase were observed, indicating that the material that composes the hillock is similar to the pristine polymer. This indicates that the formation of the hillock results basically from a physical reorganization of the molecules and does not involve significant chemical degradation. Similar results were found by Daya *et al.*[21] for TM-SFM topography images of MeV-ion-bombarded mica surfaces. It was shown that the structural arrangement on the hillock tail is similar to that found on the undamaged mica surface. Energy transport models like the pressure pulse,[26] that involve a correlated momentum transfer arising from the energy density gradient in the track, seem to be suitable to explain the observed phenomena.

TM-SFM images of PS targets of different molecular weights bombarded with 20-MeV $^{197}Au^{7+}$ and 85-MeV $^{197}Au^{9+}$ are shown in Fig. 2. Most defects present a crater followed by a hillock elongated in the direction of the ion incidence and raised regions on the crater sides (rims). The dimensions of the defects induced by the 197-MeV $^{197}Au^{20+}$ ions are similar to the ones observed for the 85-MeV $^{197}Au^{9+}$ bombardment. It can be clearly seen in Fig. 2 the different morphologies of the impact features for the various molecular weights. For a given ion energy, at low M_w the craters are large and the hillocks are tiny or absent. With increasing M_w, the craters become smaller and the deformed regions show up.

The crater length and width, c_l and c_w, respectively, for the three bombardment energies are plotted as a function of M_w in Fig. 3. A fast decrease of the crater lateral dimensions for low M_w ($<4\times10^4u$) is observed in Figs. 3(a) and 3(b). In this regime, the width of the craters is almost inversely proportional to M_w, e.g., $c_w \propto M_w^{-0.8}$ for 85-MeV ions. For higher M_w, the scaling of the surface track dimensions with M_w is less steep. The crater size remains approximately constant for $M_w > 1.6\times10^5u$ upto the highest M_w tested (2×10^7u), not shown in Fig. 3. A similar trend was observed by Eriksson *et al.*[16] in their study of MeV-ion-induced cratering on several different bio-organic films, but the saturation of the crater size occurred at lower M_w values, around 6×10^3u.

All the craters have an approximately elliptical shape, but are more rounded in low M_w samples. The length/width ratio of craters produced by the 20-MeV Au bombardment varies from 1.6 (for low M_w) to about 2 (for high M_w), while for 85-MeV and 197-MeV Au bombardments, the difference in this ratio for low and high molecular weights is even larger varying from 1.7 to about 3.

Figure 4 shows the mean hillock length (hl) and mean hillock height (hh) as a function of M_w. The lowest dimensions for hl and hh were found on the film with $M_w = 3250u$. At this M_w, some defects present a hillock, but not all of them. In Fig. 4, the average values for $M_w = 3250u$ are calculated only with the defects presenting a hillock. This

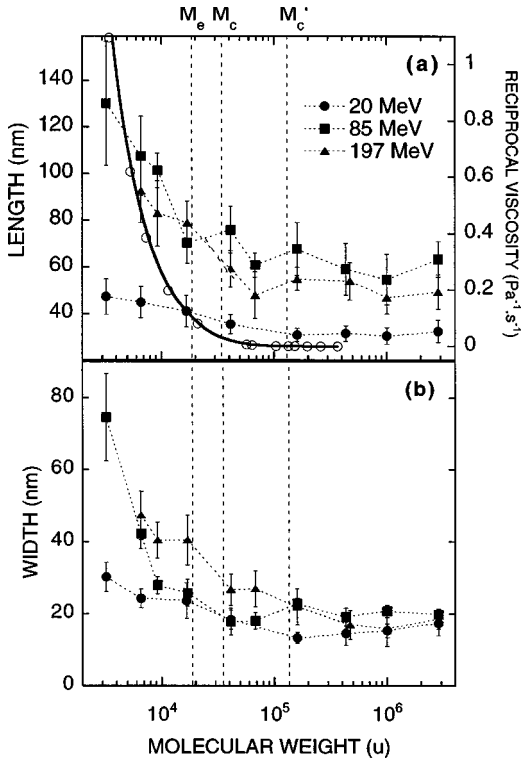

FIG. 3. Mean values of (a) crater length and (b) crater width, plotted against the PS molecular weight for samples bombarded with 20-, 85-, and 197-Mev Au ions. The solid curve in (a) shows the *reciprocal viscosity* $(1/\eta)$ as a function of M_w, for the PS (Ref. 27). The vertical dashed lines indicates the critical molecular weights (see text).

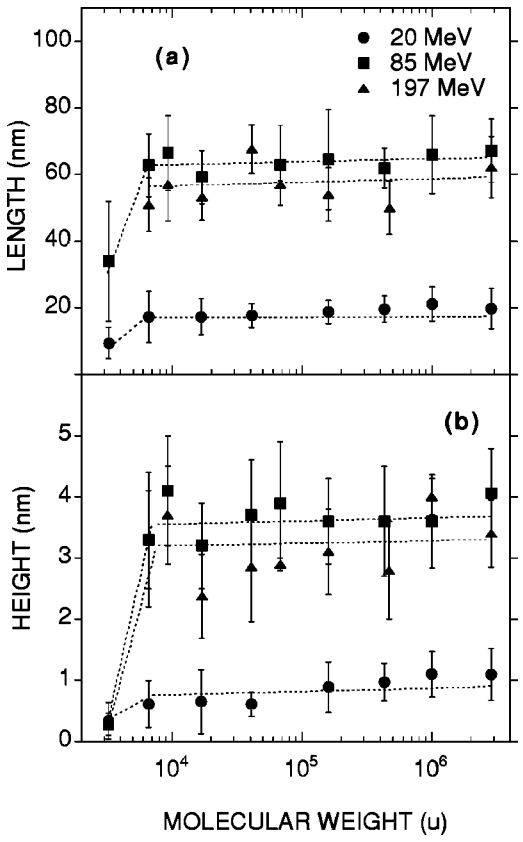

FIG. 4. Mean values of (a) hillock length and (b) hillock height, plotted against the PS molecular weight for samples bombarded with 20-, 85-, and 197-Mev Au ions.

M_w is considered a threshold for the observation of a permanent deformation (the hillock). An increase of hl and hh is observed as M_w increases and, similar to those observed for the craters, the values are approximately constant for high M_w samples.

B. Dependence on viscoelastic parameters

In order to interpret the dependence of surface track dimensions on the polymer M_w, an analysis of the dynamics of polymeric material at molecular level must be carried out. For this purpose, some well-known results from viscoelastic theory for undiluted and nearly monodisperse linear polymers in the melt are introduced below.[27,28]

For low M_w samples, the chain movement is governed by frictional forces between the monomeric units. Above a given molecular weight M_c, besides the frictional force, the entanglement of the chains, or more precisely, the entanglement coupling, must be considered. This coupling between the entanglements is caused by topological restraints that are not spatially fixed, but can be treated as a set of obstacles or a sequence of slip links.[29,30] M_c is a critical molecular weight that influences steady-flow viscosity by entanglement coupling, being related with the *entanglement molecular weight* M_e (the average molecular weight between coupling loci), but not in a simple manner.[27] For PS, $M_c(=34\,000u)$ is about two times $M_e(=17\,700u)$.

We argue that the viscosity of the films (or the frictional force plus the entanglement coupling at the molecular level) is a key parameter to understand the behavior of the crater lateral dimensions as a function of M_w. Figure 3(a) shows also the *reciprocal viscosity* $(1/\eta)$ as a function of M_w. These data were extracted from viscosity measurements of PS fractions at 217 °C, taken from Ref. 27. The viscosity presents a linear dependence on M_w, below M_c, and a $M_w^{3.4}$ dependence above M_c. The change of the scaling of the viscosity with M_w above M_c, results from the presence of entanglements between the chains, as stated before. There is a good correlation between the reciprocal viscosity curve and the observed crater size.

Besides the parameters M_e and M_c, there is also a critical molecular weight that influences the steady-state recovery compliance, called $M_c'(=130\,000u$, for PS). M_c' concerns to the average distortion of the polymer coils during flow, being an estimate of the capacity to recover from an induced deformation after the stress is ceased. For $M_w<M_c'$, the compliance is a linear function on M_w: the lower the M_w, the smaller the recovery capacity and the higher the permanent deformation (the crater) is expected to be. For $M_w>M_c'$, the compliance becomes constant (independent of M_w). This behavior of the compliance with M_w is consistent with the results in Fig. 3.

In summary, the changes in the viscosity and in the compliance with M_w favor the formation of larger craters in the

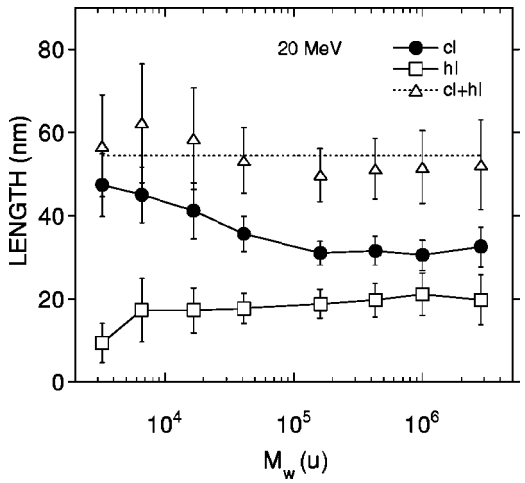

FIG. 5. Crater length (cl), hillock length (hl), and total length of the defect (cl+hl), for PS bombarded with 20-MeV $^{197}Au^{7+}$.

low molecular weight samples and explain, at least qualitatively, the reduction of the crater size as M_w increases and the saturation of the crater dimensions for $M_w > M_c'$. Considering the similarity of the curve of the reciprocal viscosity and the decrease of the crater's lateral size, the viscosity seems to be the most important parameter affecting the variation in the crater sizes on the different films.

The total size of the defects (crater plus hillock lengths) induced by 20-MeV ions is plotted as a function of M_w in Fig. 5. It is observed that the total length of the defects is approximately constant, within the estimated error. Considering the constancy of the total length of the defects, the presence of the hillocks can be interpreted as a frustration of the ejection of the molecules that appears as a plastic deformation. In samples with high M_w, the ejection is made difficult by the presence of entanglements (or enhancement of the viscosity), resulting in smaller craters (as seen before) and larger hillocks, when compared to samples of low M_w.

However, the actual scenario may be more complex. The presence of the hillocks behind the craters is an indication that the local temperature at the hillock regions is below T_g, at least for time intervals not higher than about few minutes. Otherwise, the hillocks would not be observed because the chains would quickly relax, as has been recently demonstrated by Papaléo *et al.*[22] Simple estimations of the temperature rise at a point corresponding to the hillock position using a thermal spike model[31,32] indicate that the temperatures may be higher than the polymer T_g, but for time intervals smaller than few nanoseconds.[33] This time is much smaller than the time necessary for a large-scale chain movement[27] at the temperatures indicated by the model. For example, the time necessary for a large-scale chain movement for a PS sample of 200 000*u* at 110 °C is of the order of many seconds.[27] That is, at the hillocks, the local temperature rise is small, i.e., below T_g, or higher than T_g but for a short period of time, and the polymer response is of a glass. In this case, the viscoelastic properties are dominated by short-range configurational rearrangements, which are not substantially affected by differences in M_w. This is consistent with the relative constancy of the hillock size with M_w, except for the lowest $M_w(=3250u)$. This M_w is below M_e, and has a reduced T_g ($\approx 80\,^\circ$C) as compared to the T_g of higher M_w targets (see Table I). Thus both effects, the absence of interchain constraints and the lower T_g, may explain the absence of a hillock at $M_w = 3250u$, either because of a lower effective binding field, which facilitates molecular ejection, or because of a fast relaxation of possibly formed deformations.

C. AFM operational parameters

We have performed a systematic study of the influence of the microscope operational parameters on the measured dimensions of the impact features. The cantilever-free amplitude (A_0) (amplitude value when the tip is far from the surface) and the amplitude when the tip is engaged on the sample (A) were used to determine the attenuation factor, given by $(A_0 - A)/A_0$. The A value is controlled via the feedback setpoint. The deformation exerted by the tip onto the sample (via compression, material dragging, etc.) can be estimated by doing repetitive scans over the same region, varying the feedback setpoint (i.e., the strength of tip-sample interaction) and analyzing the line profiles.[12] Also, the recovery of the deformation can be tested, measuring the line profiles going from high to low setpoint values (i.e., low to high tip-sample interaction) and returning to the initial setpoint values. In the tests, we used amplitude attenuations ranging from 0.15 to 0.40. For a PS sample with $M_w = 6600u$ the crater depth and the hillock height decreased by about 30% in this attenuation range, while the crater width increased by 10%. For a sample with higher $M_w(160\,000u)$ the same test showed significant differences: the increase in the crater width is nearly the same as for low M_w PS ($\approx 10\%$), but the crater depth remains practically unchanged, decreasing only by 3%. For the hillock height, a decrease was observed similar to that for low M_w sample—about 30%. A strong dependence of the depth of the craters on the tip shape was also observed; images taken with high-quality tips and/or tips with smaller cone angles give deeper craters. The depth of the craters measured with unusually sharp tips can be three times larger than the ones taken on the same sample with average quality tips. Similar results, and even more pronounced, were found for bombarded poly(methylmethacrylate) films.[11]

The differences between the crater depth for the low- and the high-M_w samples can possibly be understood by the facility to drag low molecular weight molecules from the surface into the crater, resulting in a shallower hole. The crater width behaves in a similar manner in the two cases suggesting that the material drag is not important in the variation of this dimension. The decrease in hillock height can be associated to a deformation due to the high pressure exerted by the tip (compression) that acted equally in the two samples. We found that the induced changes of the crater depth and width and the hillock height with the increase of tip-sample interaction are *not recoverable*, i.e., when the tip-sample interaction is decreased to lower levels, the initial values of the measured dimensions are not restored.

Permanent deformations induced by the tip on surface tracks in biomolecular samples[12] were also detected. On the

other hand, induced surface tracks in mica,[20,34] a much stronger material, were stable over a large amplitude attenuation range.

In this work the images were taken with amplitude attenuation in the 0.15–0.28 range. Under such conditions, the interaction was high enough for a stable imaging and the tip-induced deformations were relatively small, $<3\%$ for the crater width and $<15\%$ for the hillock height; for example, and imaging was stable during a complete scan.

IV. CONCLUSIONS

PS thin films with different molecular weights (3250 to 2×10^7u), were bombarded at a grazing angle by MeV ions, and characterized by scanning force microscopy in the intermittent contact mode. Phase mode imaging shows that the material that forms the hillock has similar elastic response as the pristine polymer, suggesting that a ''gentle'' energy deposition process is related to hillock formation, without a large chemical degradation. Craters' lateral dimensions are systematically reduced on films of heavier macromolecules. A fast decrease in crater area is observed in the region of low M_w ($<4\times10^4u$). In this region the crater width scales with $M_w^{-0.8}$ for 85-MeV Au ions. For higher M_w, the scaling is less steep and the craters' size remain approximately constant for $M_w>1.6\times10^5u$. The observed saturation of the crater size for high M_w values, coincides with the onset of entanglement effects in the polymer. Moreover, the lateral dimensions of the craters follow the same trend as the *reciprocal viscosity* $(1/\eta)$ when plotted against M_w, indicating that the viscosity is governing the final lateral dimensions of the craters. Hillock dimensions are roughly independent of M_w above the threshold M_w, around $3250u$ and the total length of the defects (crater plus hillock lengths) is approximately constant. The survival of the plastically deformed regions, originating in the hillocks, is an indication that the local temperature rises, due to the ion impact at these regions is insufficient to induce large-scale movements of the chains, and the polymer response is of a glass. In this case, the viscoelastic properties are dominated by short range configurational rearrangements, which are not much affected by differences in M_w.

ACKNOWLEDGMENTS

This work has been partially supported by CNPq, FINEP, and FAPERGS (Brazil).

*FAX: +55 51 319 17 62. Email address: lucio@if.ufrgs.br

[1] R. Katz, S. C. Sharma, and M. Homayoonfar, in *The Structure of Particle Tracks*, edited by F. H. Attix (Academic Press, New York, 1972), p. 317.
[2] R. L. Fleischer, P. Price, and R. M. Walker, *Nuclear Tracks in Solids* (University of California, Berkeley, 1975).
[3] R. Spohr, *Ion Tracks and Microtechnology* (Vieweg, Braunschweig, 1990).
[4] J. Kopniczky, C. T. Reimann, A. Hallén, and B. U. R. Sundqvist, Phys. Rev. B **49**, 625 (1994).
[5] R. M. Papaléo, P. Demirev, J. Eriksson, P. Håkansson, B. U. R. Sundqvist, and R. E. Johnson, Phys. Rev. Lett. **77**, 667 (1996).
[6] R. M. Papaléo, Nucl. Instrum. Methods Phys. Res. B **131**, 121 (1997).
[7] T. Venkatesan, L. Calcagno, B. S. Elman, and G. Foti, in *Ion Beam Modification of Insulators*, edited by P. Mazzoldi and G. W. Arnold (Elsevier, Amsterdam, 1987), Vol. 2, p. 301.
[8] G. Marletta, Nucl. Instrum. Methods Phys. Res. B **46**, 295 (1990).
[9] L. Calcagno, G. Compagnini, and G. Foti, Nucl. Instrum. Methods Phys. Res. B **65**, 413 (1992).
[10] R. M. Papaléo, A. Hallén, B. U. R. Sundqvist, L. Farenzena, R. P. Livi, M. A. de Araújo, and R. E. Johnson, Phys. Rev. B **53**, 2303 (1996).
[11] R. M. Papaléo, L. S. Farenzena, M. A. de Araújo, R. P. Livi, M. Alurralde, and G. Bermudez, Nucl. Instrum. Methods Phys. Res. B **148**, 126 (1999).
[12] J. Eriksson, J. Rottler, and C. T. Reimann, Int. J. Mass Spectrom. Ion Processes **175**, 293 (1998).
[13] D. D. N. B. Daya, A. Hallén, J. Eriksson, J. Kopniczky, R. M. Papaléo, C. T. Reimann, P. Håkansson, B. U. R. Sundqvist, A. Brunelle, S. Della-Negra, and Y. L. Beyec, Nucl. Instrum. Methods Phys. Res. B **106**, 38 (1995).
[14] F. Thibaudau, J. Cousty, E. Balanzat, and S. Boufard, Phys. Rev. Lett. **67**, 1582 (1991).
[15] T. Hagen, S. Grafström, J. Ackermann, R. Neumann, C. Trautmann, J. Vetter, and N. Angert, J. Vac. Sci. Technol. B **12**, 1555 (1994).
[16] J. Eriksson, J. Kopniczky, G. Brinkmalm, R. M. Papaléo, P. Demirev, C. T. Reimann, P. Håkansson, and B. U. R. Sundqvist, Nucl. Instrum. Methods Phys. Res. B **101**, 142 (1995).
[17] J. Ackermann, N. Angert, R. Neumann, C. Trautmann, M. Dischner, T. Hagen, and M. Sedlacek, Nucl. Instrum. Methods Phys. Res. B **107**, 181 (1996).
[18] C. T. Reimann, J. Kopniczky, E. Wistus, J. Eriksson, P. Håkansson, and B. U. R. Sundqvist, Int. J. Mass Spectrom. Ion Processes **151**, 147 (1995).
[19] R. M. Papaléo, L. S. Farenzena, M. A. de Araújo, and R. P. Livi, Nucl. Instrum. Methods Phys. Res. B **151**, 135 (1999).
[20] D. D. N. B. Daya, P. Demirev, J. Eriksson, A. Hallén, P. Håkansson, R. E. Johnson, J. Kopniczky, R. M. Papaléo, C. T. Reimann, J. Rottler, and B. U. R. Sundqvist, Radiat. Meas. **28**, 101 (1997).
[21] D. D. N. B. Daya, A. Hallén, P. Håkansson, B. U. R. Sundqvist, and C. T. Reimann, Nucl. Instrum. Methods Phys. Res. B **103**, 454 (1995).
[22] R. M. Papaléo, L. D. de Oliveira, L. S. Farenzena, M. A. de Araújo, and R. P. Livi, Phys. Rev. B **62**, 11 273 (2000).
[23] J. P. Cleveland, B. Anczykowski, A. E. Schmid, and V. B. Elings, Appl. Phys. Lett. **72**, 2613 (1998).
[24] G. Bar, R. Brandsch, M. Bruch, L. Delineau, and M.-H. Whangbo, Surf. Sci. Lett. **444**, L11 (2000).
[25] O. P. Behrend, L. Odoni, J. L. Loubet, and N. A. Burnham, Appl. Phys. Lett. **75**, 2551 (1999).
[26] R. E. Johnson, B. U. R. Sundqvist, A. Hedin, and D. Fenyö, Phys. Rev. B **40**, 49 (1989).
[27] J. D. Ferry, *Viscoelastic Properties of Polymers*, 3rd ed. (Wiley, New York, 1980).

[28] W. W. Graessley, in *Physical Properties of Polymers*, 2nd ed., edited by J. E. Mark, A. Eisenberg, W. W. Graessley, L. Mandelkern, E. T. Samulski, J. L. Koenig, and G. D. Wignall (American Chemical Society, Washington, D.C., 1993), Chap. 3, p. 97.

[29] P. G. De Gennes, *Scaling Concepts in Polymer Physics* (Cornell University Press, Ithaca, NY, 1979).

[30] M. Doi and S. F. Edwards, *The Theory of Polymer Dynamics* (Clarendon Press, Oxford, 1986).

[31] L. E. Seiberling, J. E. Griffith, and T. A. Tombrello, Radiat. Eff. **52**, 201 (1980).

[32] R. E. Johnson and W. L. Brown, Nucl. Instrum. Methods Phys. Res. B **198**, 103 (1982).

[33] L. S. Farenzena, R. P. Livi, and R. M. Papaléo (unpublished).

[34] J. Herbig, C. T. Reimann, M. Bergqvist, S. Oscarsson, and I. V. Vorobyova, Nucl. Instrum. Methods Phys. Res. B **149**, 119 (1999).